Negative surge in open channel: physical, numerical and analytical modelling

M. Reichstetter[1] and H.Chanson[1]
[1]School of Civil Engineering
The University of Queensland
Brisbane St Lucia, QLD 4072
AUSTRALIA
E-mail: m.reichstetter@uq.edu.au

Abstract: *Negative surges are caused by a sudden change in flow resulting from a decrease in water depth. New experiments were conducted in a horizontal channel (L = 12 m, W = 0.5 m) to record the unsteady water depth and turbulence in negative surges. The data were collected using video imagery, acoustic displacement meters and acoustic Doppler velocimetry (ADV). The experimental setup was designed to record data at two different locations within the channel under controlled flow conditions. The detailed results are compared with an analytical solution and a numerical solution of the Saint-Venant equation. The results derived from the analytical solution of the Saint-Venant equations compare well to the surface elevation data recorded from the physical experiments. The numerical solution of the Saint-Venant equations accounting for some friction compared not as well as the analytical solution implying that the effects of bed friction were small.*

Keywords: *Negative Surge, Physical Modelling, Turbulence, Numerical modelling, Analytical modelling*

1. INTRODUCTION

Dam break waves have attracted some attention during the past years. However, most studies focused on the positive surge front of the dam break wave such as Schoklitsch (1917), Dressler (1954), Lauber (1997), Chanson (2005). Only a few studies provided information on the negative surge (Lauber 1997). The physical experiments were used to validate the surge characteristics and rate of propagation. Most studies focused on qualitative observations and free surface measurements, while only few studies included some turbulence measurements.

A negative surge is an unsteady open channel flow characterised by a decrease in water depth. Negative surges can occur downstream of a control structure when the discharge is reduced. They also occur upstream of a control structure that is opened rapidly. For a stationary observer the negative surge appears to be a gentle lowering of the free surface. Based on the Saint-Venant equations, the negative surge propagates at a relative celerity of $U = (g\ d_0)^{1/2}$ in a rectangular channel, with d_0 being the initial water depth (Chanson 2004, Henderson 1966, Montes 1998). More generally, the propagation of the negative surge may be predicted using the methods of characteristics and the Saint-Venant equations (Barré de Saint Venant 1871, Henderson 1966).

In this paper, the propagation of a negative surge and its characteristics were studied. New physical experiments were conducted in a large-size laboratory facility, measuring both the unsteady free-surface profile and turbulent velocity field. The physical data provide a unique description of the negative surge and there were compared both analytical and numerical results. More generally, the data set may be used for numerical model validation.

2. EXPERIMENTAL FACITLITY AND INSTRUMENTATION

2.1. Experimental facility and instrumentation

The experiments were performed in a horizontal flume at the University of Queensland. The channel was 0.5 m wide and 12 m long, with a smooth PVC bed and glass walls. The water was supplied by a constant head tank. A fast-opening tainter gate was located at the downstream end of the channel at

x=11.15 m. Figure 1 shows some photographs of the experimental setup and the surge propagation.

(a) 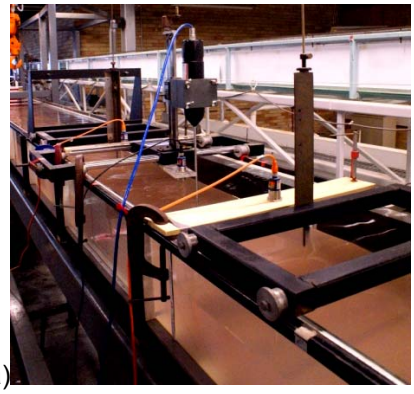 (b) 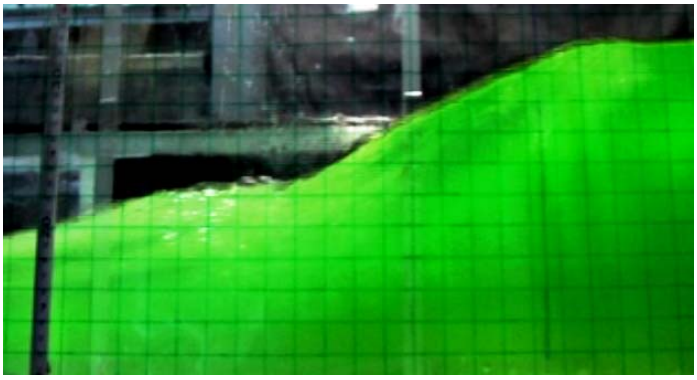

Figure 1 Photographs of the (a) experimental setup with ADV and acoustic displacement meters and (b) the negative surge propagation (from left to right) at 4.8 m upstream of the gate

The water discharge was measured with two orifice meters that were designed upon the British Standards (1943). The percentage of error was less than 2%. The unsteady water depth was measured using a series of acoustic displacement meters Microsonic™ Mic+25/ IU/TC. The data accuracy and response of the acoustic displacement meters (ADM) were 0.18 mm and 50 ms, respectively. The turbulent velocity components were measured using an acoustic Doppler velocimeter (ADV) Nortek™ Vectrino+ (Serial No. VNO 0436). The ADV had a side-looking head equipped with four receivers. The velocity rate was 1.0 m/s and the sampling rate was set at 200 Hz for all the experiments with a data accuracy of 0.01 m/s. Two series of experiments were performed to measure the unsteady free-surface profile. Figure 2 shows a schematic of the first series of experiments, where the velocity was recorded immediately upstream of the gate at x= 10.5 m, while the depth measurements were taken at, x= 10.8 m, x= 10.5 m, x= 10.2 m and x= 6 m with the acoustic displacement meters. For the second series, the velocity field was recorded at x = 6 m, while the depth measurements were taken at x= 10.8 m, x= 6.2 m, x= 6 m and x= 5.6 m. In each case, the ADV measurements were recorded at four different vertical elevations, z= 6.69 mm, z= 25.01 mm, z= 123.94 mm and z= 135.2 mm. Twenty-five negative surge experiments were conducted for each of the four vertical ADV locations. Figure 2 shows a definiton sketch with the streamwise coordinate x of origin a the upstream end of the channel and the coordinate z perpendicular to it mesured from the channel bottom. The initial channel depth is d_0, the instantaneous flow depth is d, and the initial flow velocity is V_0. The flow depth and the velocity vary with location x and time t during the negative surge propagation.

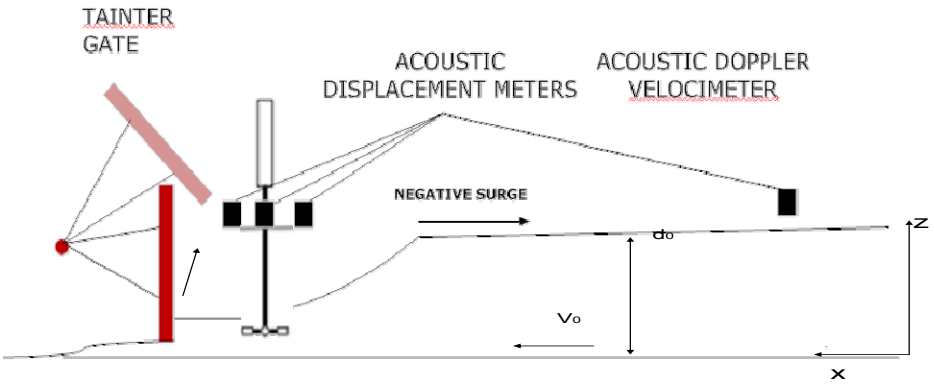

Figure 2 Sketch of experimental layout

Video imagery was used to assess the depth profile and the celerity of the passing surge. A Panasonic™ NV-H30 video camera was used to record the surge at two different locations within the channel. The first location was immediately upstream of the gate, with a full view of the gate to assess

the impact of the gate opening on the surge formation. The second location for the video recordings was about x= 6 m. The video movies were recorded at 25 frames per second for the duration of the surge. The focal plan of the camera was placed slightly beneath the initial free-surface so that the camera was facing up the surface. The slight angle of the camera meant that the recorded image showed the free surface close to the wall rather than on the channel centreline. The camera was set back approximately 0.5 m from the channel sidewall. A 20 mm grid was placed on the side wall of the channel for reference purposes and lens distortion correction. Different colour dyes were added to the water to improve the visibility of the surface edge in the images (e.g. Fig. 1b).

2.2. Inflow conditions and surge generation

The negative surges were produced by opening rapidly a tainter gate. The gate was operated manually and the opening times were less than 0.2 s. Two main series of measurement were conducted. The first series aimed to study the unsteady free surface properties using video imagery and acoustic displacement meters. The second series was related to the turbulence measurements using an ADV. During the second series the depth measurements were recorded using only the acoustic displacement meters. For all experiments, the initial discharge was 0.020 m^3/s and the initial tainter gate opening (or undershoot gap) was 30 mm. After the rapid gate opening, the gate did not intrude into the flow as sketched in Figure 2.

3. PHYSICAL AND NUMERICAL RESULTS

3.1. Observations

The surface water profiles at the gate showed a steeper drop in water depth close to the gate (e.g. x = 10.8 m) compared to the observations further upstream at x = 6 m (Fig. 3 & 4). Most velocity measurements, close to the gate, presented a spike before the surge develops, which might be related to the rapid gate opening. There was an increased turbulence in the vertical velocity component V_z data shortly after the surge formation in all the reported cases, compared to the steady state. The longitudinal velocity V_x data were closely linked with the depth profile. The transverse velocity component V_y showed little fluctuations before, during and after surge formation. The present data implied that the gate opening was an unsteady three-dimensional turbulent process.
Generally, the water depth decreased relatively gradually after the initial surge formation. The free surface measurements showed some marked curvature near the surge leading edge. The longitudinal velocity component increased at the same time as the water depth decreased. The velocity measurements at x= 6 m showed some higher fluctuations during the initial phases of the surge propagation, compared to the steady state data. The increase of turbulence observed during the negative surge propagation might indicate some significant turbulent mixing.

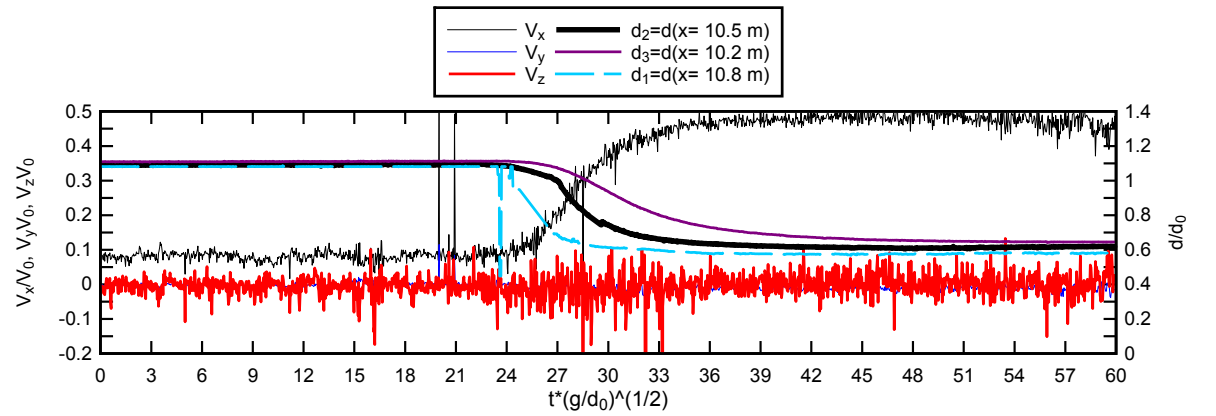

(a)

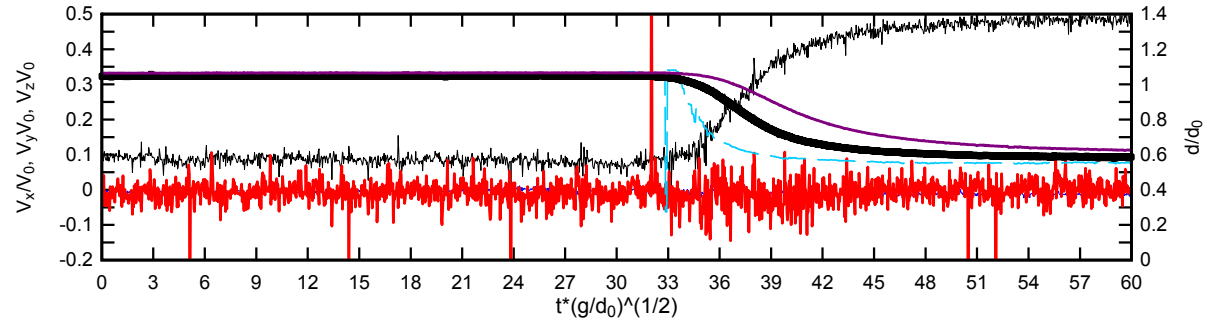

(b)

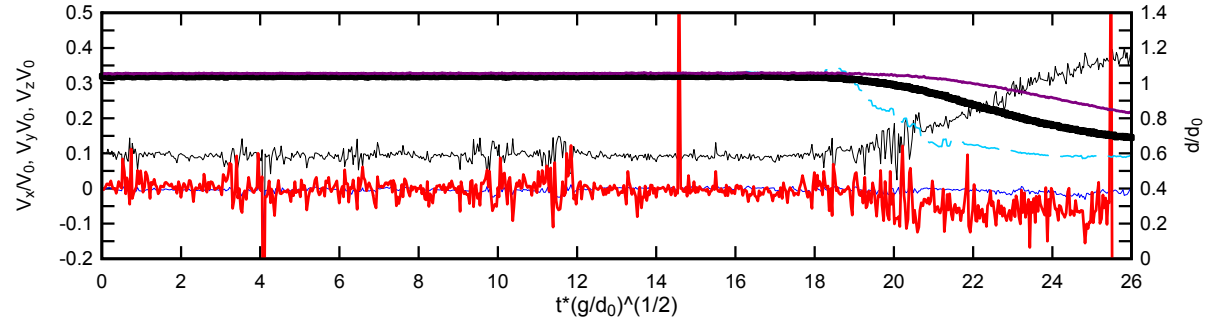

(c)

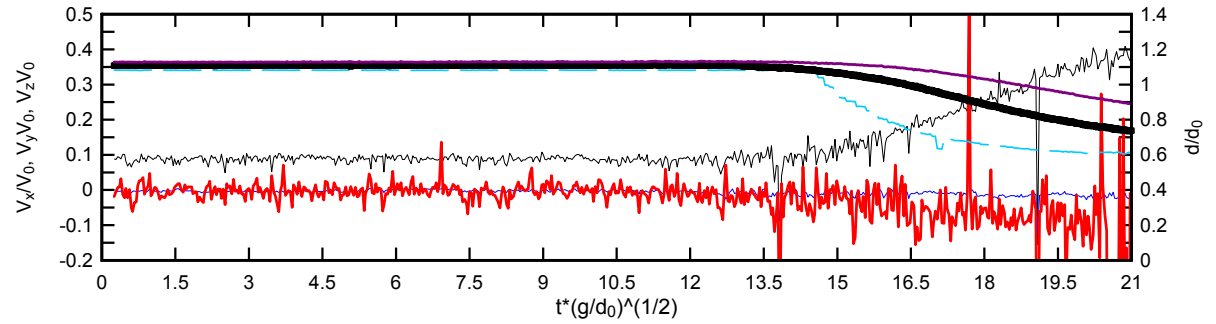

(d)

Figure 3 Dimensionless velocity and depth measurements of a negative surge: (a) x = 10.5 m, z = 6.69 mm, Q = 20 l/s, d_0 = 0.21 m and initial gate opening 30 mm; (b) x = 10.5 m, z = 25.01mm, Q = 20 l/s, d_0 = 0.21 m and initial gate opening 30 mm; (c) x = 10.5 m, z = 123.94 mm, Q = 20 l/s, d_0 = 0.21 m and initial gate opening 30mm; (d) x = 10.5 m, z = 135.2 mm , Q = 20 l/s, d_0 = 0.21 m and initial gate opening 30 mm.

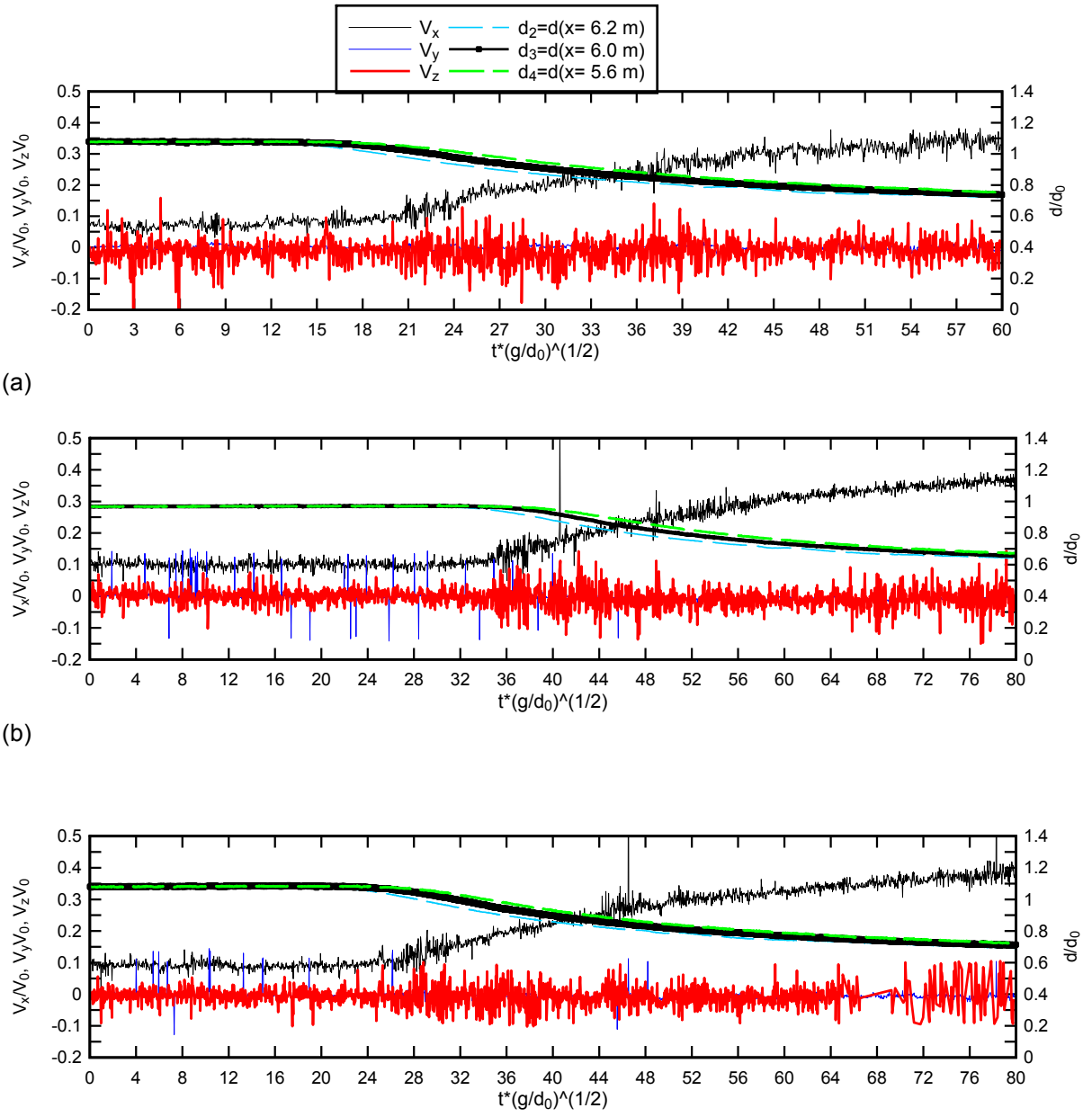

Figure 4 Dimensionless velocity and depth measurements of a negative surge: (a) x = 6 m, z = 6.69 mm, Q = 20 l/s, d_0 = 0.21 m and initial gate opening 30 mm; (b) x = 6 m, z = 123.94 mm , Q = 20 l/s, d_0 = 0.21 m and initial gate opening 30 mm; (c)) x = 6 m, z = 135.2 mm , Q = 20 l/s, d_0 = 0.21 m and initial gate opening 30 mm.

3.2. Analytical and numerical modelling

The Saint-Venant equations are applied for one-dimensional flows. Some basic assumptions include: (1) the flow is one dimensional; (2) the streamline curvature is small and the pressure distribution is hydrostatic. Considering these assumptions for unsteady flows, every point at any time during the simulation can be characterised by two variables, that is V and d where V is the velocity and d is the water depth. The following system of two partial differential equations can be used to describe the unsteady flow properties:

$$\frac{\partial d}{\partial t}+\frac{A}{B}\times\frac{\partial V}{\partial x}+V\times\frac{\partial d}{\partial x}+\frac{V}{B}\times\left(\frac{\partial A}{\partial x}\right)_{d=cons\tan t}=0 \quad (1)$$

$$\frac{\partial V}{\partial t}+V\times\frac{\partial V}{\partial x}+g\times\frac{\partial d}{\partial x}+g\times(S_f-S_o)=0 \quad (2)$$

where t is the time, A is the cross-section area, B is the free-surface width, x is the longitudinal co-ordinate positive downstream, S_o is the bed slope, θ is the angle between the bed and the horizontal, with θ> *0* for a downward slope and S_f is he friction slope. The friction slope is defined as $S_f=f/2V^2/(gD_H)$ where D_H is the hydraulic diameter (or equivalent pipe diameter) and the Darcy-Weisbach friction factor f is a non-linear function of both Reynolds number and relative roughness. Equation (1) is the differential form of the continuity equation and Equation (2) is the differential expression of the momentum equation.Some simple solutions of the Saint-Venant equations may be obtained using the "simple wave" approximation. A simple wave is defined as a wave for which $(S_o = S_f = 0)$ that has constant initial water depth and flow velocity. The characteristic system of equations for a simple wave is:

$D/Dt(V + 2C) = 0$ forward characteristic (3)

$D/Dt(V - 2C) = 0$ backward characteristic (4)

along :

$d x/dt = V + C$ forward characteristic (5)

$d x/dt = V – C$ backward characteristic (6)

where $(V + 2C)$ is a constant along the forward characteristic. For an observer moving at the absolute velocity $(V + C)$, the term $(V + 2C)$ appears constant. Correspondingly $(V - 2C)$ appears constant along the backward characteristic. When the characteristic trajectories are plotted in the (x, t) plane, they represent the path of the observers travelling on the forward and backward characteristics. For each forward characteristic, the slope of the trajectory is $1/(V + C)$ and $(V + 2C)$ *and* is constant along the characteristic trajectory. Collectively the characteristic trajectories form contour lines of $(V + 2C)$ and $(V - 2C)$ (Chanson 2004). The simple wave equations were applied to the negative surge experiments.

The numerical integration of the Saint-Venant equations was performed using the Hartree method. The Hartree method consists of a fixed grid with fixed time and time and special intervals (Montes 1998, Chanson 2004). It is also referred to as the method of specified time intervals. The flow properties are known at time t = (n-1)δt. At the following time-step t +δt, the characteristic intersection at point M (x = i δt, t = n δt) are projected backwards in time where they intersect the line t = (n-1)δt at points L and R whose locations are unknown. The characteristic system reads as follows:

$V_L + 2C_L = V_M+2C_M +g(S_f-S_0)\delta t$ forward characteristic (7)

$V_R + 2C_R = V_M-2C_M +g(S_f-S_0)\delta t$ backward characteristic (8)

$(x_m-x_L)/\delta t = V_L+C_L$ forward characteristic (9)

$(x_m-x_R)/\delta t = V_R+C_R$ forward characteristic (10)

assuming $(S_f - S_0)$ constant during the time step δt. The subscripts M, L, R refer to points in the characteristic system (Chanson 2004).

Both the analytical solution and numerical model data were compared with the physical data (Fig. 5). The video data and the ADM data presented a close agreement at x= 6 m. The data recorded by the video camera at x= 10.8 m showed some slight difference with the recorded ADM data. This might be the result of the gate opening, which was a rapidly varied flow and caused a lot of turbulence. Figure 5 shows that the analytical solution based upon the simple wave theory did give some good agreement

with the physical data (both ADM and video data). The numerical solution of the Saint-Venant equations using the Darcy friction factors f= 0.015 and f= 0.025 did not compare as well as the analytical solution nor with the physical data. The finding suggests that the bed friction has relatively little effect on the negative surge characteristics. Note that most computer softwares use the numerical solution of the Saint-Venant equations for solving one-dimensional flows. Figure 5 shows that the best agreement with the recorded ADM and video data is reached by the simple wave solution. Therefore, one may argue that the analytical solution of the Saint-Venant equation does match the physical results better than the numerical solutions. Note however that the present flume had a rectangular cross-section and was lined with PVC and glass. Therefore, the physical tests were performed with relatively smooth conditions. In natural channels, it might be required to include different friction factors to account for the natural surface roughness.

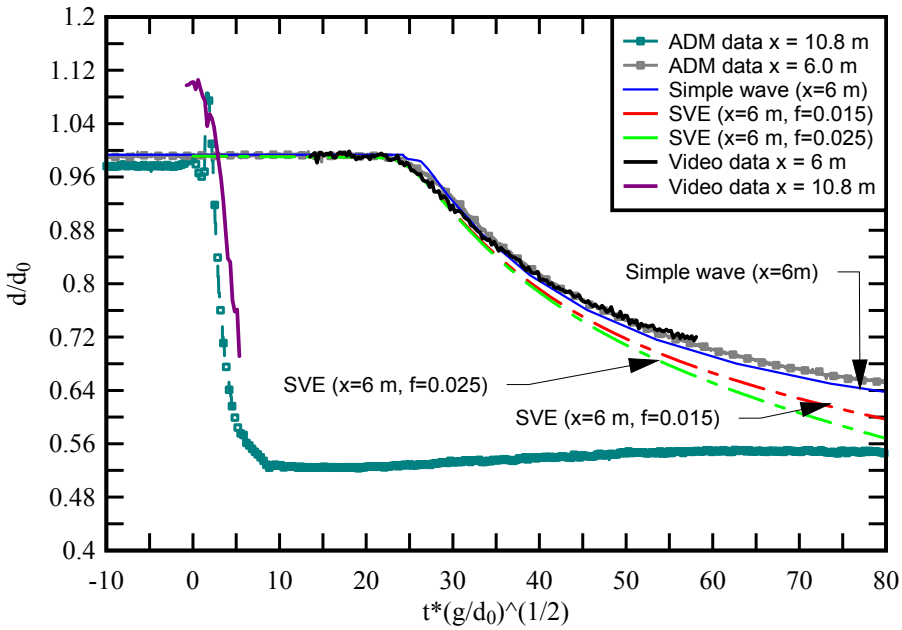

Figure 3 Dimensionless unsteady free-surface profile during the negative surge

4. CONCLUSION

Limited quantitative informations about the characteristics and propagation of negative surges were available to date. No studies known to the authors presented turbulence data in negative surges under similar experimental settings with high temporal and spatial resolutions. Herein new physical experiments were conducted carefully in a large rectangular channel to investigate specifically the unsteady free-surface profile and turbulence characteristics of a negative surge. The detailed velocity measurements were performed at high frequency (200 Hz), while the free-surface elevations were recorded using non-intrusive techniques, namely acoustic displacement meters (ADM) and video imagery. The physical data were analysed and compared to analytical and numerical solutions of the Saint-Venant equations.

The results showed that there was some increased turbulence occurring during the initial stages of surge propagation. Further there was some more intense turbulence occurring next to the gate shortly after opening, than observed further upstream. The rate of water elevation decrease was the largest at the beginning of the negative surge propagation, while the longitudinal velocity increased during the initial stages of negative surge. The results derived from the analytical solution of the Saint-Venant equations compared well to the surface elevation data recorded during the physical experiments. The numerical results accounting for boundary friction did not compare as well, and the finding implied that the negative surge propagation was relatively little affected by the boundary friction within the experimental flow conditions.

The present results suggested that the negative surge remains a challenging topic for the computational modelers. Yet one must ask: Do the results of the negative surge investigated in a laboratory setting represent the real world? Is the analytical solution of the Saint-Venant equations more applicable to derive the surface profile of the surge propagation, as compared to the numerical solutions used in the most of the one-dimensional flow models?

5. REFERENCES

Barré de Saint Venant, A.J.C. (1871), *Théorie et equations Générales du Mouvement Non Permanent des Eaux, avec Applications aux Crues des Rivières et à l'Introduction des Marées dans leur Lit (2ème Note) [Theory and equation of unsteady flows, with applications to river floods and tidal influence (2nd Note)]*. Comptes Rendus des séances de l'Académie des Science des Sciences, Paris, France. Séance, 73, 237-240.

Chanson, H. (2004). "*Environmental Hydraulics of Open Channel Flows*." Elsevier Butterworth-Heinemann, Oxford, UK.

Chanson, H. (2005). "Applications of the Saint-Venant Equations and Method of Characteristics to the Dam Break Wave Problem." Report No. CH55/05, Dept. of Civil Engineering, The University of Queensland, Brisbane, Australia, May, 135 pages.
{http://www.uq.edu.au/~e2hchans/reprints/ch5505.zip}

Dressler, R. (1954). "*Comparison of Theories and Experiments for the Hydraulic Dam-Break Wave*." Proc. Intl Assoc. of Scientific Hydrology Assemblée Générale, Rome, Italy, Vol. 3, No. 38, pp. 319–328.

Henderson, F.M. (1966). "*Open Channel Flow*." MacMillan Company, New York, USA.

Lauber, G. (1997). "*Experimente zur Talsperrenbruchwelle im glatten geneigten Rechteckkanal*." Ph.D. thesis, VAW-ETH, Zürich, Switzerland (in German).

Montes, J.S. (1998). "*Hydraulics of Open Channel Flow*." ASCE Press, New-York, USA, 697 pages.

Schoklitsch, A. (1917). "*Ueber Dammbruchwellen.*" Sitzungsberichte der Kaiserlichen Akademie Wissenschaften, Viennal, Vol. 126, 1489–1514.